analytical chemistry

Article

Cite This: *Anal. Chem.* 2018, 90, 2055−2062

pubs.acs.org/ac

New Mechanism of Extractive Electrospray Ionization Mass Spectrometry for Heterogeneous Solid Particles

S. Kumbhani,[†] T. Longin,[‡] L. M. Wingen,[†] C. Kidd,[†] V. Perraud,[†] and B. J. Finlayson-Pitts*[,†]

[†]Department of Chemistry, University of California−Irvine, Irvine, California 92697-2025, United States

[‡]Department of Chemistry, University of Redlands, Redlands, California 92373, United States

Supporting Information

ABSTRACT: Real-time in situ mass spectrometry analysis of airborne particles is important in several applications, including exposure studies in ambient air, industrial settings, and assessing impacts on visibility and climate. However, obtaining molecular and 3D structural information is more challenging, especially for heterogeneous solid or semisolid particles. We report a study of extractive electrospray ionization mass spectrometry (EESI-MS) for the analysis of solid particles with an organic coating. The goal is to elucidate how much of the overall particle content is sampled, and determine the sensitivity of this technique to the surface layers. It is shown that, for $NaNO_3$ particles coated with glutaric acid (GA), very little of the solid $NaNO_3$ core is sampled compared to the GA coating, whereas for GA particles coated with malonic acid (MA), significant signals from both the MA coating and the GA core are observed. However, conventional ESI-MS of the same samples collected on a Teflon filter (and then extracted) detects much more core material compared to EESI-MS in both cases. These results show that, for the experimental conditions used here, EESI-MS does not sample the entire particle but, instead, is more sensitive to surface layers. Separate experiments on single-component particles of $NaNO_3$, GA, or citric acid show that there must be a kinetics limitation to dissolution that is important in determining EESI-MS sensitivity. We propose a new mechanism of EESI solvent droplet interaction with solid particles that is consistent with the experimental observations. In conjunction with previous EESI-MS studies of organic particles, these results suggest that EESI does not necessarily sample the entire particle when solid, and that not only solubility but also surface energies and the kinetics of dissolution play an important role.

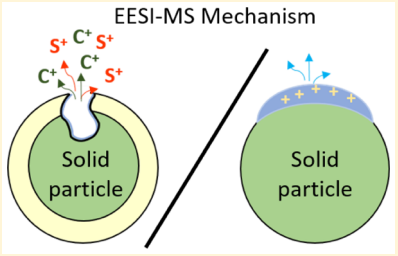

The feasibility of extractive electrospray ionization mass spectroscopy (EESI-MS), which has come into widespread use,[1,2] was first demonstrated about 20 years ago when gases were ionized by mixing the gas stream with the flow of ESI droplets.[3,4] It has since been used to explore a variety of analytes in the gas phase and in solid and liquid particles.[2,5,6] In EESI-MS, a solvent (typically a mixture of water, alcohol, and a weak acid) is directed through a charged capillary toward the entrance of a mass spectrometer, just as in conventional electrospray ionization mass spectrometry (ESI-MS). However, the analyte is not mixed with the solvent as in ESI but rather meets the stream of charged solvent droplets near the entrance to the mass spectrometer. Separating the solvent from the analyte has the advantage that the sample can be generated and studied in situ with little or no processing. A variety of organic and inorganic compounds have been studied via EESI-MS, ranging from aerosolized aqueous solutions[7] to very complicated matrices such as urine,[1] milk,[1] honey,[8] human breath,[9−13] perfume,[14,15] explosives,[16,17] drugs,[18] a variety of foods and food components,[19−24] electronic cigarette particles,[25] secondary organic aerosol (SOA), and other atmospherically relevant samples.[26−30] EESI-MS and similar approaches have also been used to study reaction intermediates[31] and follow reaction kinetics,[32−34] demonstrating the capability of this technique to study reactions in real time.

Previous studies on the detection of gases by EESI-MS suggest that the mechanism involves a gas-phase ion−molecule ionization.[35,36] However, it is not entirely clear how the solvent droplets formed by the EESI solvent spray interact with liquid or solid particles. Figure 1 is a schematic of four proposed mechanisms of interaction between EESI spray droplets (green) and liquid analyte droplets (red), adapted from the work of Wang et al.[37] In general, interactions between two droplets are dependent on many factors, including surface tensions/energies, viscosities, and the relative sizes and the

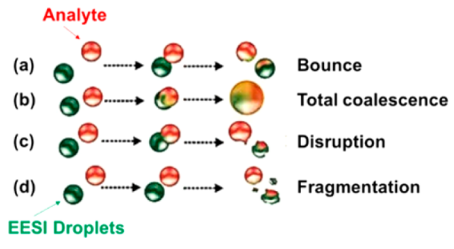

Figure 1. Schematic of proposed EESI-MS mechanisms for liquids. Adapted from Wang et al.[37]

Received: October 10, 2017
Accepted: December 21, 2017
Published: January 11, 2018

DOI: 10.1021/acs.analchem.7b04164
Anal. Chem. 2018, 90, 2055−2062

kinetic energies of the droplets.[38,39] Total coalescence (Figure 1, path b), in which the particles completely dissolve in the electrospray droplet, is one possibility. Zenobi and co-workers[40] explored the interaction of liquid droplets containing dissolved analyte with EESI solvent droplets and observed that the signal strength of the analyte was dependent strongly on its solubility in the EESI solvent. They also concluded that total coalescence of the analyte with the EESI spray droplet is not the major process, which was confirmed in a combined experimental and theoretical study.[37] Furthermore, they calculated that the solvent and sample droplets have <5 μs to interact, so a partial extraction process must occur quickly.[37] This could occur via three types of interactions between the analyte and EESI droplet: bounce, disruption, or fragmentation. The bounce mechanism (Figure 1, path a) involves the transfer of some of the analyte to the EESI droplet during the low kinetic energy collision, without much disruption of either. Alternatively, the collision could be sufficiently energetic that both the ESI droplet and the particle are significantly distorted when they separate into two droplets, the "disruption" mechanism (Figure 1, path c). Finally, in the mechanism favored by Wang et al.,[37] the collision results in fragmentation of the EESI droplet into many droplets during the transfer of some of the analyte (Figure 1, path d).

EESI-MS is very promising for real-time, in situ analysis of atmospheric particles,[26−30] since no collection or extraction is needed. However, particles in the atmosphere can be liquid, solid, or semisolid, and they can have nonuniform composition, including solid cores with an organic coating.[41−51] In order to interpret EESI-MS spectra of such particles, it is important to know how much of the particle is probed. If EESI-MS was more sensitive to the surface than to the bulk, at least under some conditions, it would provide an approach to investigating the heterogeneous nature of such particles. On the other hand, if it provided information on the average composition of the entire particle, as suggested by a linear relationship between signal intensity and mass in a model system,[27] it could also be very useful. In either event, it is important to understand what controls this, i.e., to elucidate the mechanism of interaction of the EESI solvent droplets with such particles.

To explore this issue, we prepared different two-component systems with selected composition designed to provide insight into the EESI droplet−particle interaction, and specifically, how much of the particles is sampled. The systems chosen for in-depth study were (1) glutaric acid ($HOOC(CH_2)_3COOH$, GA) coated on solid particles of sodium nitrate ($NaNO_3$) as the core; and (2) malonic acid ($HOOCCH_2COOH$, MA) coated on glutaric acid particles as the core. In addition, a few studies were carried out using succinic or adipic acid ($HOOC(CH_2)_nCOOH$, n = 2 or 4) coated on sodium chloride (NaCl) and $NaNO_3$ particles. Some studies of single component $NaNO_3$ or citric acid particles were also carried out for comparison to glutaric acid particles. The inorganic components are often found in ambient particles, such as fresh or aged sea salt.[52,53] Similarly, dicarboxylic acids and multifunctional acids are common components of particles in both field and laboratory settings.[54−61] Additional reasons for these particular choices are discussed below, in conjunction with the results. Based on these studies, we propose a new mechanism for EESI-MS analysis of solid particles that should be useful in applying this technique to complex atmospheric systems.

MATERIALS AND METHODS

A schematic diagram of the apparatus is shown in Figure S-1 in the Supporting Information (SI). The particles used as the core materials ($NaNO_3$, glutaric acid, citric acid) were generated with a constant output atomizer (TSI, Model 3076). As discussed below, in separate studies, glutaric acid was also used as a coating material. A solution (0.1% w:v for $NaNO_3$ and 4.3 mM for each organic) of the core component in 18 MΩ cm water (Milli-Q, Millipore Corporation) was atomized with nitrogen (Praxair, UHP, 99.999%), and the flow exiting the atomizer at 1.7 L min^{-1} was passed through two silica gel diffusion dryers, which resulted in low relative humidity (RH) values of the particle stream. For example, the RH of the glutaric acid particle flow after the dryers was <5%. The resulting particles were sent through the linear portion of a glass "T", which formed the main part of the coating assembly. Special care was taken to change the desiccant in the diffusion dryers every 4−5 h of run time, to ensure that the particles were dry. Each coating material (malonic acid, succinic acid, glutaric acid, and adipic acid) was heated in a cell that was attached to the lower arm of the coating assembly and carried into the linear portion with a flow of N_2 (0.5−1 L min^{-1}). The temperature of the cell was controlled by heating tape and a variable power transformer and monitored by a thermocouple inserted between the heating tape and the outer wall of the glass cell. Some of the organic vapor from the heated cell condensed onto the particles and the mixture of gases and coated particles was carried into a glass chamber (50 cm long × 2 cm outer diameter (OD) maintained at room temperature and then into a 10 cm honeycomb monolith carbon denuder (Novacarb; Mast Carbon, Ltd.) to remove the remaining organic gas. A reference experiment was carried out where the organic gas (without the core particles) from the heated cell was passed through the denuder and measured with EESI-MS. No gas-phase signal was observed, confirming that the denuder efficiently removed the gas-phase organic material. From the denuder, the coated particles flowed either to intersect the stream of EESI droplets as described earlier[26,62] or to a scanning mobility particle sizer (SMPS) to measure the particle size distribution (see the SI).

Increasing amounts of coating were generated by increasing the temperature of the coating material in the cell. This increased the gas-phase concentration to which the core particles were exposed and, hence, the amount of coating on the particles. Although the SMPS measurements did not provide definitive data on coating thickness because of the nature of the polydisperse distribution and thin coatings, as shown below, the mass spectrometry data consistently exhibit increasing organic coating signals with increased coating temperatures. The coating material was not detected when the particles passed through an empty coater or at low temperatures where the vapor pressure of the coating material was too low to provide sufficient gas-phase concentrations for condensation on the particles. The temperature at which the coating materials self-nucleate to form undesired particles was determined in separate experiments by increasing the temperature of the coating cell until a significant number (a few hundred/cm^3) of particles appeared. The maximum temperature for coating was then kept at least 5 °C below the self-nucleating temperature.

The EESI solvent was a 1:1 (v:v) mixture of methanol (ACS grade, Sigma−Aldrich) and 18 MΩ cm water that was made

DOI: 10.1021/acs.analchem.7b04164
Anal. Chem. 2018, 90, 2055−2062

slightly acidic by the addition of 0.2%−1% (v:v) of formic acid (Certified ACS, 88%, Fisher Scientific). This EESI solvent mixture was injected into a 100 μm ID silica capillary (IDEX Health & Science or Postnova Analytics) at typical flow rates of 30−80 μL h^{-1}, using a syringe pump (NE 1000, New Era Pump Systems, Inc.). A positive potential of 4.0−4.9 kV was applied to the capillary from an external power supply (Model 248, Keithley) to generate charged solvent droplets ∼1 cm away from a triple quadrupole mass spectrometer inlet (API-300, AB Sciex). Varying the voltages and solvent flow rates was necessary when the capillary burst and had to be recut or replaced, since each new capillary produced a stable Taylor cone at a slightly different flow rate−voltage combination, as confirmed using a microscope. A curtain plate voltage of +1 kV was used on the mass spectrometer. The instrument was mass-calibrated using conventional ESI-MS with a standard calibration mixture of poly(ethylene glycol) with an average molecular weight (MW) of 200 Da (PEG-200, Sigma−Aldrich). All measurements were performed in the positive-ion mode, and Analyst 1.2 software (AB Sciex) was used to acquire the mass spectra and time profile data.

To account for background signal from contamination in the sample lines and in the air around the curtain plate of the mass spectrometer,[62] the sample flow was replaced with an identical flow of nitrogen gas. Mass spectra of the nitrogen background were recorded for several minutes (usually 2−4) and these spectra were averaged. The average background spectrum was subtracted from the average sample spectrum for the EESI spectra. All subtractions were performed in Igor Pro (Wavemetrics, Inc.). In addition, single-ion monitoring was used in some experiments to provide better sensitivity for specific ions. For comparison, ESI spectra of the coated particles were also acquired. Details of the collection and extraction can be found in the SI. No subtractions were carried out for ESI data.

The coating materials used in this study were as follows: malonic acid (MW 104 Da; Sigma−Aldrich, >99%), succinic acid (MW 118 Da, Sigma−Aldrich BioXtra, >99%), glutaric acid (MW 132 Da; Sigma−Aldrich, 99%), and adipic acid (MW 146 Da; Sigma−Aldrich, BioXtra, >99.5%). The core materials included sodium nitrate (FW 85 Da, Fisher Scientific, Certified ACS grade, >99%), sodium chloride (FW 58 Da, Fisher Scientific, Certified ACS grade, 99.9%), and citric acid (MW 192 Da, Fisher Scientific, Certified ACS grade, 99%). Note that, in some experiments, glutaric acid was also used as a core. All solids were used as received.

RESULTS AND DISCUSSION

EESI-MS was used to probe a polydisperse distribution of particles consisting of a solid $NaNO_3$ core (a typical size distribution is given in Figure S-2 in the SI) coated with different amounts of glutaric acid obtained by maintaining the temperature of the coating assembly between 50−80 °C, depending on the desired amount of coating. Sodium nitrate was chosen as the core, since it is highly soluble in water at room temperature (∼11 M)[63] and high solubilities are important for EESI-MS analysis, based on earlier EESI-MS studies.[27,28,40] Glutaric acid itself is also quite soluble in water at room temperature (∼4 M)[64] and has sufficient vapor pressure (1.7×10^{-4} Pa)[65] for coating the particles. If the EESI solvent extracts the core, $NaNO_3$ should readily dissolve and provide Na^+ ions to form adducts with the glutaric acid, assuming the solubilities of the $NaNO_3$ and glutaric acid are as high in the EESI solvent as in water. For example, ESI-MS of glutaric acid (Figure S-3 in the SI) shows that, upon the addition of Na^+ ions, essentially all of the signal is found in the form of sodium adducts $[M + Na]^+$ at m/z 155, as expected, given the great sensitivity of ESI-MS to the presence of sodium.[66] However, if only the surface layers are extracted into the solvent droplets and not the $NaNO_3$ core, there would not be a significant contribution from sodium adducts of glutaric acid to the mass spectrum.

Figure 2a shows the EESI mass spectrum of glutaric acid coated on $NaNO_3$ particles at 50 °C, the lowest temperature for

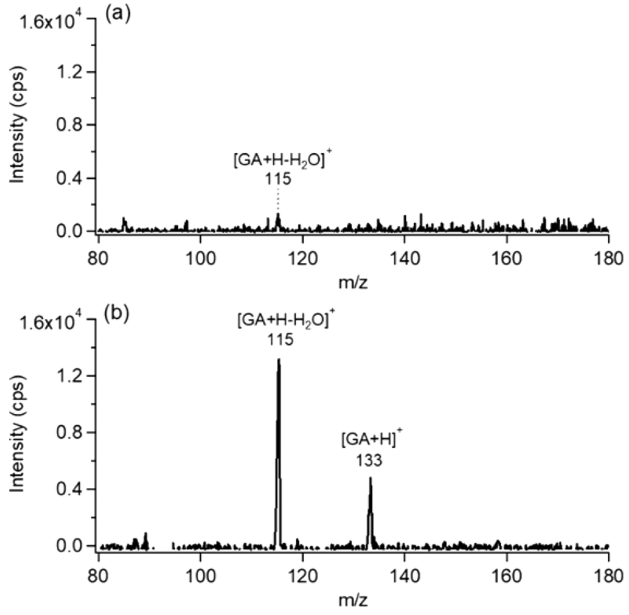

Figure 2. EESI-MS spectra of glutaric acid (GA) coated on sodium nitrate particles where the coating temperature was (a) 50 °C, to give a thin coating, or (b) 80 °C, to give a thicker coating.

which any coating signal was observed, and Figure 2b at 80 °C, the highest temperature which could be confidently used to avoid self-nucleation of the glutaric acid. Signals at m/z 133 and 115, corresponding to glutaric acid $[M + H]^+$ and $[M + H - H_2O]^+$ ions, respectively, are clearly present at 80 °C (Figure 2b) but are very small for the coating formed at the lower temperature (Figure 2a). This is more evident in Figure S-4 in the SI, which shows increasing glutaric acid signals using single-ion monitoring, as a function of the temperature of the coating assembly and, hence, the amount of coating. At the lower temperatures (Figure 2a), the signals are similar in magnitude to the background signal, but as seen in the inset in Figure S-4, there is an increase in the signals in switching from the background to the coated particles. Under all conditions, the peak at m/z 155 due to the sodium adduct is small and does not change significantly with the amount of coating (note that, as discussed below, while dry $NaNO_3$ particles are not detectable, they can be detected if the particles are wet). These data suggest that the entire particle is not dissolving, since a significant sodium adduct peak is not observed for any coating thickness.

Some experiments were also carried out using dry NaCl as the core, and the results for glutaric-acid-coated NaCl particles were similar, i.e., there was a small sodium adduct signal, but only the glutaric acid signal increased with temperature of the coating cell. Dry NaCl particles coated with succinic acid or adipic acid were also briefly studied. While the results were

DOI: 10.1021/acs.analchem.7b04164
Anal. Chem. 2018, 90, 2055−2062

qualitatively consistent with the glutaric acid experiments, the signals due to the organics were much smaller, as expected due to their much lower aqueous solubilities (0.6 and 0.2 M, respectively, at room temperature).[64] In addition to solubility, other parameters might contribute to the lack of signal observed in these cases, as discussed below.

For comparison to the EESI-MS of coated particles, the $NaNO_3$ particles coated with glutaric acid were also sampled onto Teflon filters immediately after the EESI measurements, extracted as described in the SI and the resulting solutions were used to obtain ESI mass spectra. Complete dissolution of the coated particles is expected to show the particle composition as a whole and, given the high solubility of both glutaric acid and $NaNO_3$, all of the particle components should be readily observed. If the mass spectrum obtained in this manner is the same as that from EESI-MS, it would establish that EESI-MS was also dissolving the entire particle. Figures 3a and 3b show

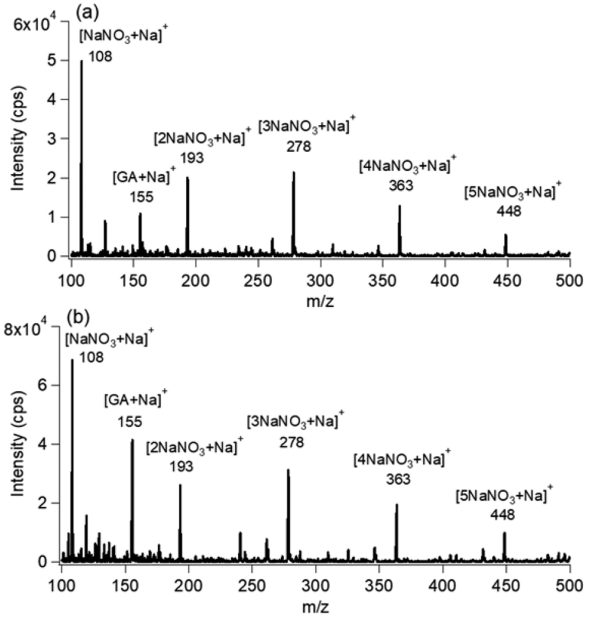

Figure 3. ESI-MS spectra of glutaric acid (GA) coated on sodium nitrate particles, where the coating temperature was (a) 50 °C, to give a thin coating, (b) 80 °C, to give a thicker coating. The particles were collected on filters and dissolved in acidified methanol:water (50:50) solvent before ESI-MS spectra were obtained.

the ESI mass spectra of the extracted particles corresponding to the samples in Figures 2a and 2b. The sodium nitrate core in ESI mass spectra manifests itself in a series of peaks corresponding to clusters of the salt with Na^+ ions, e.g., $[(NaNO_3)_nNa]^+$ where $n = 1$ is represented by the peak at m/z 108, $n = 2$ is represented by the peak at m/z 193, etc. A peak due to the sodium adduct of the glutaric acid at m/z 155 is evident for the lowest temperature/thinnest coating (Figure 3a), and it increases with coating temperature/thickness (Figure 3b). All of the glutaric acid is in the form of sodium adducts and no peaks for $[GA + H]^+$ are observed, suggesting that sodium is not the limiting reagent in formation of the adduct when the entire particle is sampled.

The differences between the spectra obtained by EESI-MS for particles sampled on the fly and by ESI-MS for a sample collected on a filter and extracted are striking. The ESI-MS spectra for particles completely dissolved in solution show prominent peaks for the sodium adducts of glutaric acid and numerous peaks for sodium nitrate clusters (see Figures 3a and 3b). If these particles were completely dissolved by the solvent spray in EESI-MS, then the resulting spectra should show similar peaks. However, the EESI-MS spectra (Figure 2) show no peaks for sodium nitrate clusters and only very small peaks for the sodium adducts (Figure S-4 in the SI). The contrast in these spectra indicate that the entire particle is not dissolving when the solid particle interacts with the EESI droplets.

An ESI-MS spectrum of a $NaNO_3$ solution in the absence of glutaric acid, in which the same $[(NaNO_3)_nNa]^+$ cluster peaks are observed, is presented in Figure S-5a in the SI. For comparison, EESI-MS of wet $NaNO_3$ particles was also carried out. In this case, the wet $NaNO_3$ particles/droplets formed in the atomizer were directed into the EESI region directly, bypassing the diffusion dryers, coating assembly, and denuder. Figure S-5b in the SI shows that the same clusters of $[(NaNO_3)_nNa]^+$ are clearly observed. However, no signal was observed for dry $NaNO_3$ by EESI-MS. Disruption of the surface of liquid and/or wet particles appears to be facilitated, compared to the dry surface, allowing penetration of the EESI droplets into the particles.

Given this comparison between the EESI and ESI spectra, and in light of the high solubilities of both the core and coating constituents, there must be factors other than bulk solubility that come into play in determining the small sodium adduct signal observed for dry, coated, solid $NaNO_3$ particles in EESI-MS. These include (1) the possibility that the electrospray droplets are only probing the outermost surface layers of the particles even at the thinnest coatings; and/or (2) solid $NaNO_3$ is not efficient in providing Na^+ ions to form the adducts with the glutaric acid coating. Given the very small organic signals at the lowest coating temperature, it seems unlikely that the electrospray droplets would not sample at least some of the core.

The second explanation, i.e., that Na^+ ions in the core are not readily available, seems most likely and may arise from a combination of factors. First, bulk solubility, which is clearly important in EESI,[27,28,40] is determined by thermodynamic equilibrium. However, dissolution may be kinetically limited, i.e., there may not be sufficient time to disrupt the $NaNO_3$ surface and dissolve the core prior to the MS inlet. Chemical reactions are often much faster in small droplets compared to bulk solution.[67] If the same was true for dissolution processes in the present system, the generation of Na^+ ions and their adducts would have been favored, which is clearly not the case.

A second factor limiting the availability of sodium from the $NaNO_3$ core involves the nature of the interaction of the electrospray solvent with the solid salt. If the sodium embedded in the core surface layer cannot be easily mobilized, it will not be available for forming adducts with the diacid as happens when the Na^+ ions are freely available in solution. However, this would again suggest that the core itself is not dissolving. Finally, a third possibility is that the diacid forms a salt with $NaNO_3$ ($Na^+{}^-OOC(CH_2)_3COO^-Na^+$), and this forms a barrier that prevents or slows penetration into the core. Although the reaction in aqueous solution is known to form the salt,[68] the sodium salts of the diacids were observed to be quite soluble, as seen in the ESI-MS spectra and hence do not seem likely to form such a barrier. In short, the EESI droplets clearly do not sample much of the dry $NaNO_3$ core, whether coated or uncoated with glutaric acid, indicating that factors other than

DOI: 10.1021/acs.analchem.7b04164
Anal. Chem. 2018, 90, 2055−2062

bulk solubility can be important in determining sensitivity to EESI-MS for heterogeneous solid particles.

To further probe the mechanism, particles of glutaric acid were generated as the core (see Figures S-6a and S-6b in the SI for a typical size distribution and EESI-MS spectrum). They were coated with malonic acid which has a high aqueous solubility at room temperature (6 M)[64] and sufficient vapor pressure (1.7×10^{-4} Pa)[65] to provide a good coating. The temperature range over which malonic acid could be heated without decomposition was limited to 70 °C. The EESI-MS spectrum of pure malonic acid particles (Figure 4a) was first obtained and shows peaks at m/z 105, 87, and 122, corresponding to $[M + H]^+$, $[M + H - H_2O]^+$ and $[M + NH_4]^+$, characteristic of malonic acid.

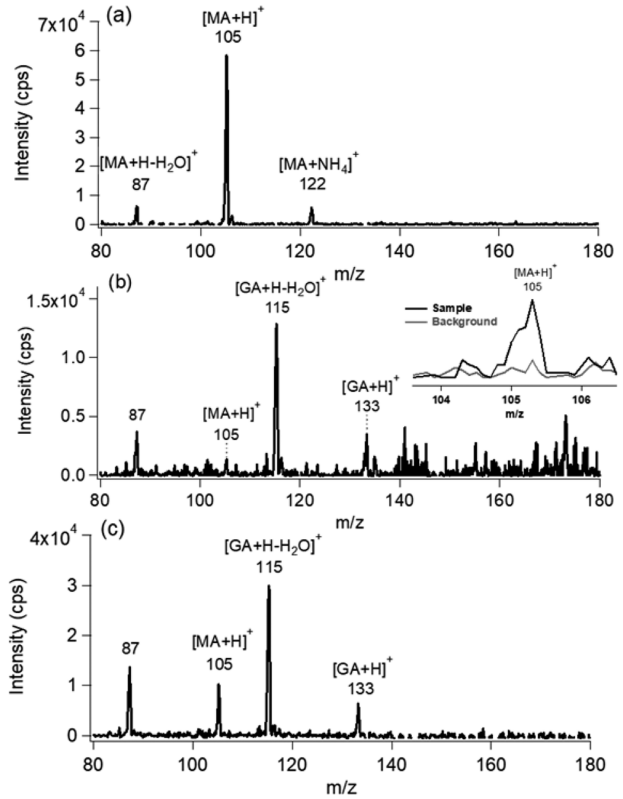

Figure 4. EESI-MS spectra of (a) malonic acid (MA) particles; (b) malonic acid coated on glutaric acid (GA) particles at 50 °C, to give a thin coating; (c) malonic acid coated on glutaric acid particles at 70 °C to give a thicker coating. The inset in panel (b) shows there is no malonic acid detected in the background, with small but detectable levels in the sample at 50 °C.

Figures 4b and 4c show the EESI-MS spectra of glutaric acid particles coated with malonic acid heated at 50 and 70 °C, respectively. The malonic acid signal at m/z 105 increases with coating temperature, relative to those for the glutaric acid core signal, as expected (the same is true of m/z 87 but there is also a contribution from glutaric acid at this mass). However, in contrast to the case of glutaric acid on $NaNO_3$, the glutaric acid core is now clearly sampled at both amounts of coating. The particles were again collected for ESI-MS analysis and the corresponding ESI mass spectra are shown in Figures 5a and 5b. Comparing the EESI-MS (Figure 4) to the ESI-MS (Figure 5) at the same temperatures shows that much more of the glutaric acid core is observed in ESI-MS, as expected for

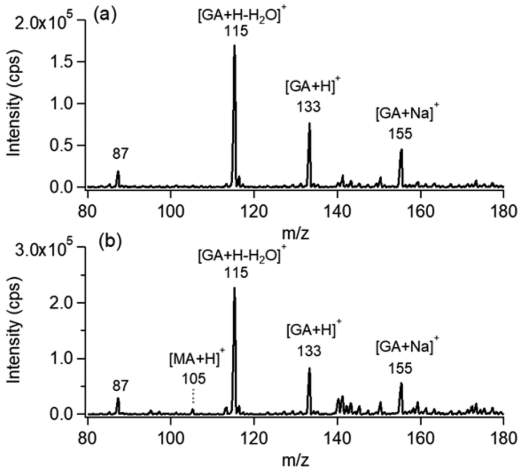

Figure 5. ESI-MS spectra of malonic acid (MA) coated on glutaric acid (GA) particles, where the coating temperature was (a) 50 °C, to give a thin coating, or (b) 70 °C, to give a thicker coating. The particles were collected on filters and dissolved in acidified methanol:water (50:50) solvent before ESI-MS spectra were obtained.

complete dissolution of the particles in the ESI solvent during extraction. For example, at 70 °C, the ratio of the $[M + H]^+$ signals for the core glutaric acid to the malonic acid coating is 0.6 in EESI but 9 in ESI. Clearly only part of the core is being sampled by EESI-MS.

To explain the experimental data, we propose a new mechanism shown schematically in Figure 6. The first step is adsorption of the charged EESI droplets onto the surface of the solid particle. The size of the droplets initially exiting the capillary is on the order of 1 μm but they rapidly shrink (within 5 μs)[37] due to evaporation and fission. It is likely that in these experiments the EESI droplets at the point of intersection are smaller than the particles[37] whose size extends out to ~0.6 μm (see the SI). If the surface of the particle is soluble in the EESI solvent, the EESI droplet will start to dissolve into the surface (paths a and b). This creates a "crater" in the particle surface layer while the solvent continues to evaporate from the charged droplet, concentrating the charge in the crater. Then, there are two possibilities, depending on the nature of the core. In path a, the core is not significantly penetrated on these time scales, whereas in path b, the droplet penetrates the core. In either case, when the droplet reaches its Rayleigh limit and undergoes Coulombic explosion, it carries with it some of the material immediately adjacent to the exploding droplet in the crater. The depth of penetration of the adsorbed droplet will be dependent not only on bulk solubility (which is an equilibrium phenomenon) but also on how easily the surface of the solid can be disrupted to start the dissolution process (which is kinetically determined). However, if the surface is not easily penetrated by the solvent, the charged droplet can spread on the particle, dispersing the charges and inhibiting significant ionization of the analyte (path c). Note that although the coated particles are shown as a core–shell configuration in Figure 6, the coating may not be uniform. However, elemental mapping using scanning electron microscopy of $NaNO_3$ particles coated with glutaric acid at 80 °C showed the carbon was co-located with sodium, nitrogen, and oxygen (see Figure S-7 in the SI), suggesting that the organic is distributed over the $NaNO_3$ particle. In any event, uneven distribution would not change the model or conclusions.

DOI: 10.1021/acs.analchem.7b04164
Anal. Chem. 2018, 90, 2055−2062

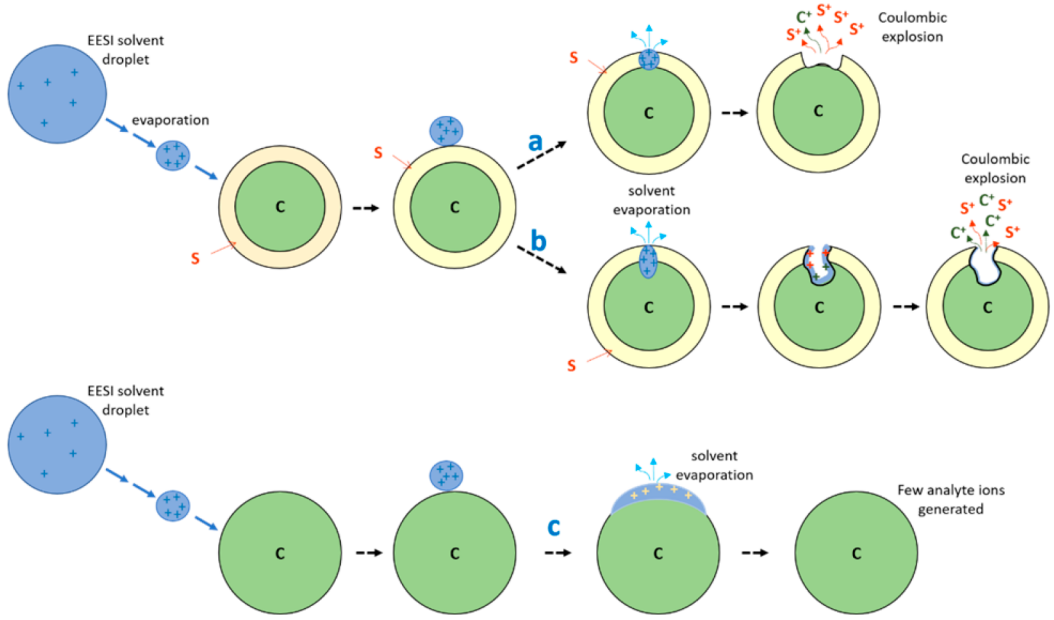

Figure 6. Schematic of proposed EESI mechanism for solid particles. S = coating material, C = core material. Note that it is likely that the particles in the experiments (which extend to 0.6 μm in diameter) are larger than the impinging EESI droplets. S^+ represents ions formed from surface coating molecules, S, including $[S + H]^+$, $[S + H - H_2O]^+$, and $[S + H - H_2O - CO]^+$. C^+ represents ions formed from reaching the core of the particle, including $[S + Na]^+$ in the case of $NaNO_3$ core or $[C + H]^+$, $[C + H - H_2O]^+$, and $[C + H - H_2O - CO]^+$ in the case of organic cores where C is a molecule from the core of the particle.

Glutaric acid cores and coatings were easily observed by EESI-MS. On the other hand, the lack of signals from the dry $NaNO_3$ core either alone or diacid-coated suggests that disruption of the $NaNO_3$ surface and formation of a "crater" did not occur, at least on the time scale of the droplet–particle interactions. While the core would be expected to dissolve, based on bulk solubility, it clearly did not.

This proposed EESI mechanism for solids is different from that proposed for liquid analytes (Figure 1) in that adsorption of the liquid EESI droplet on the solid surface is the initial step and further mixing of the charged solvent droplet with the analyte is dependent on how easily the surface is disrupted in the interaction. This adds a kinetics aspect to the sensitivity of the technique, in addition to the well-known importance of solubility.[27,28,40] The ease of surface penetration by the EESI droplet reflects differences in surface free energy, defined as the work required to form a unit area of surface.[69] Vapor pressures are related to surface free energies and, hence, provide a measure of the ease of disruption of the surface.[70,71] The vapor pressure of glutaric acid at room temperature is 1.7×10^{-4} Pa,[65] clearly much greater than for the solid $NaNO_3$ salt, indicative of a higher surface free energy for the organic acid. As a result, penetration into the less-stable surface of glutaric acid should be faster, in effect digging a "crater" in the surface. In the case of a more-stable solid particle surface such as dry $NaNO_3$, penetration may not be as fast and the EESI droplet may then initially spread across the surface. If this is the case, then the charges may be less concentrated than in the case of the crater mechanism, and either carry less of the underlying material with them when they explode or may not undergo repulsive Coulombic explosion at all. This may be responsible for the lack of EESI-MS signal from dry $NaNO_3$ particles.

Consistent with this, there are some organics whose surfaces are not as readily disrupted as glutaric acid (and malonic acid) on the time scale for interaction with EESI droplets, resulting in much less sensitivity in EESI-MS compared to glutaric acid. This is the case, for example, with citric acid, which has a strongly hydrogen-bonded structure.[72,73] Although the citric acid solubility in water (~6 M)[64] is similar to that of glutaric acid, its room-temperature vapor pressure (3.8×10^{-5} Pa)[74] is lower, consistent with a lower surface free energy and, hence, more-stable surface. However, the presence of small amounts of water (generated by bypassing the diffusion dryers) improved the signal intensities (see Figure S-8 in the SI). This also supports the proposed mechanism, in that water is known to mobilize surface species[75] and, hence, facilitate disruption of the surface. The low EESI-MS signals observed in experiments on succinic or adipic acids on NaCl could also be explained by their lower surface free energies,[70] as indicated by their lower vapor pressures (7.7×10^{-5} Pa and 1.9×10^{-5} Pa, respectively),[65] in addition to their much lower solubilities in the EESI solvent.[64]

Overall, these studies are consistent with earlier studies that showed the importance of solubility for analysis using EESI-MS.[27,28,40] However, our results show that solubility alone may not be the sole parameter governing the EESI process for solid particles.

The use of coated particles demonstrates that our EESI-MS system does not sample the entire particle. Previous studies of tartaric acid particles[27] showed that there was a linear dependence of the signal on mass, rather than surface area, which was interpreted as the total dissolution of the particles. In the context of our proposed mechanism, this could be the case for the homogeneous, highly soluble, small particles used in that study, where the EESI solvent flow was also approximately an order of magnitude higher than that used here. In that case, there may have been many more EESI droplets and/or larger droplets impinging on a smaller surface area,[37] forming many craters and deep craters that, in effect, led to sampling of the entire particle. Another contributing factor could be the contact time between the EESI solvent drops and the analyte particles; this is not well-defined for these systems, but if it was longer in

DOI: 10.1021/acs.analchem.7b04164
Anal. Chem. 2018, 90, 2055–2062

those studies, there would be more time to disrupt the surface prior to the mass spectrometer entrance.

CONCLUSIONS

EESI-MS is clearly a very promising, but somewhat complex, technique. As shown here, the sensitivity to various analytes may be dependent not only on their bulk solubility in the EESI solvent, but also on kinetic factors that determine whether dissolution occurs on the time scales over which the solvent droplets and particles are in contact. This provides a potential opportunity to selectively probe particles having heterogeneous composition and structure, as demonstrated here. On the other hand, the experimental conditions for EESI-MS may be adjustable to sample the entire particle under appropriate conditions. More work is needed to explore this and the proposed mechanism shown in Figure 6 in more detail.

ASSOCIATED CONTENT

Supporting Information

The Supporting Information is available free of charge on the ACS Publications website at DOI: 10.1021/acs.analchem.7b04164.

Schematic diagram of the experimental apparatus; description of particle collection and size distribution measurements; typical size distribution of dry uncoated $NaNO_3$ particles; ESI-MS spectrum of glutaric acid solution in the absence and presence of Na^+ ions; EESI-MS single-ion monitoring intensities from glutaric-acid-coated $NaNO_3$ particles as a function of coating temperature; ESI-MS spectrum of a $NaNO_3$ solution and EESI-MS spectrum of wet $NaNO_3$ particles; typical size distribution and EESI-MS spectrum of uncoated glutaric acid particles; SEM of dry $NaNO_3$ particles coated with glutaric acid; EESI-MS spectra of dry glutaric acid particles, dry citric acid particles, and wet citric acid particles (PDF)

AUTHOR INFORMATION

Corresponding Author

*Tel.: (949) 824-7670. E-mail: bjfinlay@uci.edu.

ORCID

T. Longin: 0000-0003-3193-4124

B. J. Finlayson-Pitts: 0000-0003-4650-168X

Notes

The authors declare no competing financial interest.

ACKNOWLEDGMENTS

This work was supported by the Army Research Office (No. W911NF-17-1-0105) and the National Science Foundation (No. 1647386). We thank Kjertan Lyster and Crisand Anderson for assistance with preliminary experiments, Cyril McCormick and Ricardo Jimenez for technical assistance with the mass spectrometer, and Dr. Jian-Guo Zheng and Dr. Yongjun Huo for SEM assistance. SEM analyses were performed at the UC Irvine Materials Research Institute (IMRI).

REFERENCES

(1) Chen, H.; Venter, A.; Cooks, R. G. *Chem. Commun.* **2006**, *19*, 2042−2044.

(2) Domin, M.; Cody, R. *Ambient Ionization Mass Spectrometry*; Royal Society of Chemistry: London, England, 2015.

(3) Lee, C. Y.; Shiea, J. *Anal. Chem.* **1998**, *70*, 2757−2761.

(4) Hong, C. M.; Tsai, F. C.; Shiea, J. *Anal. Chem.* **2000**, *72*, 1175−1178.

(5) Huang, M. Z.; Cheng, S. C.; Cho, Y. T.; Shiea, J. *Anal. Chim. Acta* **2011**, *702*, 1−15.

(6) Javanshad, R.; Venter, A. R. *Anal. Methods* **2017**, *9*, 4896−4907.

(7) Forbes, T. P. *Rapid Commun. Mass Spectrom.* **2015**, *29*, 19−28.

(8) Huang, X. Y.; Fang, X. W.; Zhang, X.; Dai, X. M.; Guo, X. L.; Chen, H. W.; Luo, L. P. *Anal. Bioanal. Chem.* **2014**, *406*, 7705−7714.

(9) Chen, H.; Wortmann, A.; Zhang, W.; Zenobi, R. *Angew. Chem., Int. Ed.* **2007**, *46*, 580−583.

(10) Berchtold, C.; Bosilkovska, M.; Daali, Y.; Walder, B.; Zenobi, R. *Mass Spectrom. Rev.* **2014**, *33*, 394−413.

(11) Ding, J. H.; Yang, S. P.; Liang, D. P.; Chen, H. W.; Wu, Z. Z.; Zhang, L. L.; Ren, Y. L. *Analyst* **2009**, *134*, 2040−2050.

(12) Gamez, G.; Zhu, L. A.; Disko, A.; Chen, H. W.; Azov, V.; Chingin, K.; Kramer, G.; Zenobi, R. *Chem. Commun.* **2011**, *47*, 4884−4886.

(13) Pan, S. S.; Tian, Y.; Li, M.; Zhao, J. Y.; Zhu, L. L.; Zhang, W.; Gu, H. W.; Wang, H. D.; Shi, J. B.; Fang, X.; Li, P. H.; Chen, H. W. *Sci. Rep.* **2015**, *5*, 8725.

(14) Chingin, K.; Chen, H.; Gamez, G.; Zhu, L.; Zenobi, R. *Anal. Chem.* **2009**, *81*, 2414−2414.

(15) Chingin, K.; Chen, H.; Gamez, G.; Zhu, L.; Zenobi, R. *Anal. Chem.* **2009**, *81*, 123−129.

(16) Tam, M.; Hill, H. H. J. *Anal. Chem.* **2004**, *76*, 2741−2747.

(17) Gu, H. W.; Yang, S.; Li, J.; Hu, B.; Chen, H.; Zhang, L.; Fei, Q. *Analyst* **2010**, *135*, 779−788.

(18) Gu, H. W.; Hu, B.; Li, J. Q.; Yang, S. P.; Han, J.; Chen, H. W. *Analyst* **2010**, *135*, 1259−1267.

(19) Chen, H. W.; Zenobi, R. *Chimia* **2007**, *61*, 843−843.

(20) Zhu, L.; Gamez, G.; Chen, H.; Chingin, K.; Zenobi, R. *Chem. Commun.* **2009**, 559−561.

(21) Law, W. S.; Chen, H. W.; Ding, J. H.; Yang, S. P.; Zhu, L.; Gamez, G.; Chingin, K.; Ren, Y. L.; Zenobi, R. *Angew. Chem., Int. Ed.* **2009**, *48*, 8277−8280.

(22) Law, W. S.; Chen, H. W.; Balabin, R.; Berchtold, C.; Meier, L.; Zenobi, R. *Analyst* **2010**, *135*, 773−778.

(23) Zhu, L. A.; Hu, Z.; Gamez, G.; Law, W. S.; Chen, H. W.; Yang, S. P.; Chingin, K.; Balabin, R. M.; Wang, R.; Zhang, T. T.; Zenobi, R. *Anal. Bioanal. Chem.* **2010**, *398*, 405−413.

(24) Wu, Z. C.; Chingin, K.; Chen, H. W.; Zhu, L.; Jia, B.; Zenobi, R. *Anal. Bioanal. Chem.* **2010**, *397*, 1549−1556.

(25) Garcia-Gomez, D.; Gaisl, T.; Barrios-Collado, C.; Vidal-de-Miguel, G.; Kohler, M.; Zenobi, R. *Chem. - Eur. J.* **2016**, *22*, 2452−2457.

(26) Doezema, L. A.; Longin, T.; Cody, W.; Perraud, V.; Dawson, M. L.; Ezell, M. J.; Greaves, J.; Johnson, K. R.; Finlayson-Pitts, B. J. *RSC Adv.* **2012**, *2*, 2930−2938.

(27) Gallimore, P. J.; Kalberer, M. *Environ. Sci. Technol.* **2013**, *47*, 7324−7331.

(28) Horan, A. J.; Gao, Y.; Hall, W. A., IV; Johnston, M. V. *Anal. Chem.* **2012**, *84*, 9253−9258.

(29) Gallimore, P. J.; Giorio, C.; Mahon, B. M.; Kalberer, M. *Atmos. Chem. Phys. Discuss.* **2017**, 1.

(30) Gallimore, P. J.; Griffiths, P. T.; Pope, F. D.; Reid, J. P.; Kalberer, M. *J. Geophys. Res.* **2017**, *122*, 4364−4377.

(31) Marquez, C. A.; Wang, H.; Fabbretti, F.; Metzger, J. O. *J. Am. Chem. Soc.* **2008**, *130*, 17208−17209.

(32) Zhu, L.; Gamez, G.; Chen, H. W.; Huang, H. X.; Chingin, K.; Zenobi, R. *Rapid Commun. Mass Spectrom.* **2008**, *22*, 2993−2998.

(33) McCullough, B. J.; Bristow, T.; O'Connor, G.; Hopley, C. *Rapid Commun. Mass Spectrom.* **2011**, *25*, 1445−1451.

(34) Lee, J. K.; Kim, S.; Nam, H. G.; Zare, R. N. *Proc. Natl. Acad. Sci. U. S. A.* **2015**, *112*, 3898−3903.

(35) Meier, L.; Schmid, S.; Berchtold, C.; Zenobi, R. *Eur. J. Mass Spectrom.* **2011**, *17*, 345−351.

DOI: 10.1021/acs.analchem.7b04164
Anal. Chem. 2018, 90, 2055−2062

(36) Rioseras, A. T.; Gaugg, M. T.; Martinez-Lozano Sinues, P. *Anal. Methods* **2017**, *9*, 5052−5057.
(37) Wang, R.; Gröhn, A. J.; Zhu, L.; Dietiker, R.; Wegner, K.; Günther, D.; Zenobi, R. *Anal. Bioanal. Chem.* **2012**, *402*, 2633−2643.
(38) Focke, C.; Kuschel, M.; Sommerfeld, M.; Bothe, D. *Int. J. Multiphase Flow* **2013**, *56*, 81−92.
(39) Orme, M. *Prog. Energy Combust. Sci.* **1997**, *23*, 65−79.
(40) Law, W. S.; Wang, R.; Hu, B.; Berchtold, C.; Meier, L.; Chen, H.; Zenobi, R. *Anal. Chem.* **2010**, *82*, 4494−4500.
(41) Adachi, K.; Buseck, P. R. *Atmos. Chem. Phys.* **2008**, *8*, 6469−6481.
(42) Falkovich, A. H.; Schkolnik, G.; Ganor, E.; Rudich, Y. *J. Geophys. Res.* **2004**, *109*, D02208.
(43) Hallquist, M.; Wenger, J. C.; Baltensperger, U.; Rudich, Y.; Simpson, D.; Claeys, M.; Dommen, J.; Donahue, N. M.; George, C.; Goldstein, A. H.; Hamilton, J. F.; Herrmann, H.; Hoffmann, T.; Iinuma, Y.; Jang, M.; Jenkin, M. E.; Jimenez, J. L.; Kiendler-Scharr, A.; Maenhaut, W.; McFiggans, G.; Mentel, T. F.; Monod, A.; Prevot, A. S. H.; Seinfeld, J. H.; Surratt, J. D.; Szmigielski, R.; Wildt, J. *Atmos. Chem. Phys.* **2009**, *9*, 5155−5236.
(44) Rudich, Y.; Donahue, N. M.; Mentel, T. F. *Annu. Rev. Phys. Chem.* **2007**, *58*, 321−352.
(45) Semeniuk, T. A.; Wise, M. E.; Martin, S. T.; Russell, L. M.; Buseck, P. R. *Atmos. Environ.* **2007**, *41*, 6225−6235.
(46) Wheeler, M. J.; Bertram, A. K. *Atmos. Chem. Phys.* **2012**, *12*, 1189−1201.
(47) Bauer, S. E.; Ault, A. P.; Prather, K. A. *J. Geophys. Res.* **2013**, *118*, 9834−9844.
(48) O'Brien, R. E.; Wang, B.; Kelly, S. T.; Lundt, N.; You, Y.; Bertram, A. K.; Leone, S. R.; Laskin, A.; Gilles, M. K. *Environ. Sci. Technol.* **2015**, *49*, 4995−5002.
(49) You, Y.; Bertram, A. K. *Atmos. Chem. Phys.* **2015**, *15*, 1351−1365.
(50) Buseck, P. R.; Adachi, K.; Gelencsér, A.; Tompa, E.; Pósfai, M. *Aerosol Sci. Technol.* **2014**, *48*, 777−788.
(51) Posfai, M.; Axisa, D.; Tompa, E.; Freney, E.; Bruintjes, R.; Buseck, P. R. *Atmos. Res.* **2013**, *122*, 347−361.
(52) Gard, E. E.; Gross, D. S.; Hughes, L. S.; Allen, J. O.; Morrical, B. D.; Fergenson, D. P.; Diemers, T.; Galli, M. E.; Johnson, R. J.; Cass, G. R.; Prather, K. A. *Science* **1998**, *279*, 1184−1187.
(53) Laskin, A.; Iedema, M. J.; Cowin, J. P. *Environ. Sci. Technol.* **2002**, *36*, 4948−4955.
(54) Fraser, M. P.; Cass, G. R.; Simoneit, B. R. T. *Environ. Sci. Technol.* **2003**, *37*, 446−453.
(55) Kawamura, K.; Ikushima, K. *Environ. Sci. Technol.* **1993**, *27*, 2227−2235.
(56) Kawamura, K.; Imai, Y.; Barrie, L. A. *Atmos. Environ.* **2005**, *39*, 599−614.
(57) Limbeck, A.; Kraxner, Y.; Puxbaum, H. *J. Aerosol Sci.* **2005**, *36*, 991−1005.
(58) Saarikoski, S.; Carbone, S.; Decesari, S.; Giulianelli, L.; Angelini, F.; Canagaratna, M.; Ng, N. L.; Trimborn, A.; Facchini, M. C.; Fuzzi, S.; Hillamo, R.; Worsnop, D. *Atmos. Chem. Phys.* **2012**, *12*, 8401−8421.
(59) Alves, C. A.; Pio, C. A. *J. Braz. Chem. Soc.* **2005**, *16*, 1017−1029.
(60) Koch, S.; Winterhalter, R.; Uherek, E.; Kolloff, A.; Neeb, P.; Moortgat, G. K. *Atmos. Environ.* **2000**, *34*, 4031−4042.
(61) Satsumabayashi, H.; Kurita, H.; Yokouchi, Y.; Ueda, H. *Atmos. Environ., Part A* **1990**, *24*, 1443−1450.
(62) Kumbhani, S.; Wingen, L. M.; Perraud, V.; Finlayson-Pitts, B. J. *Rapid Commun. Mass Spectrom.* **2017**, *31*, 1659−1668.
(63) Eysseltova, J.; Zbranek, V.; Skripkin, M. Y.; Sawada, K.; Tepavitcharova, S. *J. Phys. Chem. Ref. Data* **2017**, *46*, 013103.
(64) Yalkowsky, S. H.; He, Y.; Jain, P. *Handbook of Aqueous Solubility Data*, Second Edition; CRC Press: Boca Raton, FL, 2010.
(65) Bilde, M.; Barsanti, K.; Booth, M.; Cappa, C. D.; Donahue, N. M.; Emanuelsson, E. U.; McFiggans, G.; Krieger, U. K.; Marcolli, C.; Topping, D.; Ziemann, P.; Barley, M.; Clegg, S.; Dennis-Smither, B.; Hallquist, M.; Hallquist, A. M.; Khlystov, A.; Kulmala, M.; Mogensen, D.; Percival, C. J.; Pope, F.; Reid, J. P.; Ribeiro da Silva, M. A. V.; Rosenoern, T.; Salo, K.; Soonsin, V. P.; Yli-Juuti, T.; Prisle, N. L.; Pagels, J.; Rarey, J.; Zardini, A. A.; Riipinen, I. *Chem. Rev.* **2015**, *115*, 4115−4156.
(66) Greaves, J.; Roboz, J. *Mass Spectrometry for the Novice*; CRC Press: Boca Raton, FL, 2014.
(67) Badu-Tawiah, A. K.; Eberlin, L. S.; Ouyang, Z.; Cooks, G. R. *Annu. Rev. Phys. Chem.* **2013**, *64*, 481−505.
(68) Wang, B.; Laskin, A. *J. Geophys. Res.* **2014**, *119*, 3335−3351.
(69) Adamson, A. W.; Gast, A. P. *Physical Chemistry of Surfaces*; John Wiley & Sons: New York, 1997.
(70) Bilde, M.; Svenningsson, B.; Monster, J.; Rosenorn, T. *Environ. Sci. Technol.* **2003**, *37*, 1371−1378.
(71) Tao, Y.; McMurry, P. H. *Environ. Sci. Technol.* **1989**, *23*, 1519−1523.
(72) Glusker, J. P.; Minkin, J. A.; Patterson, A. L. *Acta Crystallogr., Sect. B: Struct. Crystallogr. Cryst. Chem.* **1969**, *25*, 1066−1072.
(73) Groen, H.; Roberts, K. J. *J. Phys. Chem. B* **2001**, *105*, 10723−10730.
(74) Huisman, A. J.; Krieger, U. K.; Zuend, A.; Marcolli, C.; Peter, T. *Atmos. Chem. Phys.* **2013**, *13*, 6647−6662.
(75) Allen, H. C.; Laux, J. M.; Vogt, R.; Finlayson-Pitts, B. J.; Hemminger, J. C. *J. Phys. Chem.* **1996**, *100*, 6371−6375.

DOI: 10.1021/acs.analchem.7b04164
Anal. Chem. 2018, 90, 2055−2062